



Neuronal SIRT1 regulates metabolic and reproductive function and the response to caloric restriction.

Emily Rickert, Marina O. Fernandez, Irene Choi, Michael Gorman, Jerrold M. Olefsky, and Nicholas J.G. Webster

Journal of the Endocrine Society **Endocrine Society**

Submitted: October 01, 2018 Accepted: December 19, 2018 First Online: December 24, 2018

Advance Articles are PDF versions of manuscripts that have been peer reviewed and accepted but not yet copyedited. The manuscripts are published online as soon as possible after acceptance and before the copyedited, typeset articles are published. They are posted "as is" (i.e., as submitted by the authors at the modification stage), and do not reflect editorial changes. No corrections/changes to the PDF manuscripts are accepted. Accordingly, there likely will be differences between the Advance Article manuscripts and the final, typeset articles. The manuscripts remain listed on the Advance Article page until the final, typeset articles are posted. At that point, the manuscripts are removed from the Advance Article page.

DISCLAIMER: These manuscripts are provided "as is" without warranty of any kind, either express or particular purpose, or non-infringement. Changes will be made to these manuscripts before publication. Review and/or use or reliance on these materials is at the discretion and risk of the reader/user. In no event shall the Endocrine Society be liable for damages of any kind arising references to, products or publications do not imply endorsement of that product or publication.

Neuronal SIRT overexpression impairs metabolism and fertility

Neuronal SIRT1 regulates metabolic and reproductive function and the response to caloric restriction.

Emily Rickert^{2,5}, Marina O. Fernandez^{2,6}, Irene Choi¹, Michael Gorman⁴, Jerrold M. Olefsky¹, and Nicholas J.G. Webster 1,2,3

¹VA San Diego Healthcare System, San Diego CA 92161, the ²Department of Medicine, the ³Moores Cancer Center, and the ⁴Department of Psychology, University of California San Diego, La Jolla, CA, 92093.

ORCiD numbers:

0000-0002-3827-5750

Webster

Nicholas

Received 01 October 2018. Accepted 19 December 2018.

⁵Current address: BioMendics, LLC, 4209 State Route 44, Rootstown, Ohio 44272

⁶Current address: Laboratory of Neuroendocrinology, Instituto de Biología y Medicina Experimental, CONICET. Vuelta de Obligado 2490, C1428ADN, Buenos Aires, Argentina

Sirt1 is a NAD-dependent class III deacetylase that functions as a cellular energy sensor. In addition to its well-characterized effects in peripheral tissues, emerging evidence suggests that neuronal Sirt1 activity plays a role in the central regulation of energy balance and glucose metabolism. In this study we generated mice expressing an enzymatically inactive form (N-MUT) or wild-type SIRT1 (N-OX) in mature neurons. Both N-OX male and female mice showed impaired glucose tolerance, and N-MUT female, but not male, mice showed improved glucose tolerance compared to WT littermates. Furthermore, all mice showed improved glucose tolerance with caloric restriction (CR), but the N-OX mice showed the greatest change and now showed better glucose tolerance than their littermates. At the reproductive level, N-OX females showed impaired estrous cycles, with increased cycle length and more time in estrus. LH and progesterone surges were absent on the evening of proestrus in the N-OX mice suggesting a defect in spontaneous ovulation, which was confirmed by the ovarian histology with a reduced number of corpora lutea. Despite this defect, the mice were still fertile when mated to wild-type mice on the day of pro-estrus indicating that the mice can respond to normal pheromonal or environmental cues. When subjected to CR, the N-OX mice went into diestrus arrest earlier than their littermates. Together, these results suggested that the overexpression of SIRT1 rendered the mice more sensitive to the metabolic improvements and suppression of reproductive cycles by CR, which was independent of circadian rhythms.

INTRODUCTION:

Sirtuin 1 (Sirt1) was first identified as a mammalian homolog of the yeast Silent Information Regulator 2 (Sir2) protein, which is essential for lifespan extension due to caloric restriction. The sirtuins are class III histone deacetylases that require NAD+ for enzyme activity and these enzymes function as cellular energy sensors sensitive to the intracellular NAD+/NADH ratio.

Sirt1 is activated during fasting to increase fatty acid oxidation and gluconeogenesis, and suppress insulin secretion, insulin action, and adipogenesis²⁻⁴. Conversely, SIRT1 is reduced in adipose tissue by over-nutrition in both mouse models and human obesity, and also in many brain regions⁵⁻⁸. Consequently, global transgenic overexpression improves glucose tolerance and insulin sensitivity even on a low fat diet due to increased brown adipose tissue (BAT) activity, enhanced $\beta 3$ adrenergic stimulation and reduced inflammation ⁹⁻¹¹. The global knockout is difficult to interpret as most mice die in utero or perinatally ¹²⁻¹⁴, and those that survive on an outbred background are runted¹⁴. The global inactivation of the acetylase activity by deletion of exon 4 leads to a similar phenotype with embryonic lethality but the few surviving animals showed higher triglycerides, higher fatty acid release from adipose tissue and greater hepatic steatosis on a high fat diet^{15,16}. Similarly, introduction of a point mutation (H355Y) that inactivates the enzyme activity causes runting, elevated oxygen consumption and male infertility¹⁷, and increased the susceptibility to HFD-induced metabolic dysfunction¹⁸. SIRT1 has also been reported to have tissue specific effects. Forced reduction of Sirt1 in white adipose tissue (WAT) by anti-sense oligonucleotides or conditional knockout reduced body weight and WAT weight, but increased macrophage infiltration, while overexpression prevents these effects¹⁹. Loss of Sirt1 in skeletal muscle reduces insulin sensitivity during caloric restriction²⁰. Deletion in hepatocytes causes increased hepatic glucose production, fasting hyperglycemia, greater fasting-induced steatosis, and the development of late-onset obesity 16,21-23. A transgenic overexpressing line that uses the entire Sirt1 gene did not mimic intermittent fasting, despite enhancing brown adipose tissue function and protecting against HFD-induced glucose intolerance ^{10,11,24-26}. Conflicting results have been obtained at the reproductive level. One study reported that the few surviving male mice from the global knockout studies are infertile as are the majority of female mice¹⁴, but another study found that mice could be fertile^{27,28}. Sirt1 is expressed in spermatogonia and has been implicated in germ cell development in males^{29,30}. In the ovary, SIRT1 is expressed in large follicles particularly in the oocyte and granulosa cells. Loss of SIRT1 causes small ovaries with early stage follicular development but no evidence of ovulation 14,31. SIRT1 modulates both androgen receptor and estrogen receptor-alpha function that may underlie some of the reproductive effects ³²⁻³⁵. Sirt1 thus has beneficial effects in multiple tissues to ameliorate insulin resistance and support reproduction.

SIRT1 also pays a role in the central nervous system but the results are less clear. Many studies have focused on the role of SIRT1 to prevent neuronal injury in ischemic stroke, alzheimers, brain injury and other models of neurodegeneration, potentially by reducing neuroinflammation³⁶⁻³⁸. SIRT1 also modulates cognitive function, synaptic plasticity and learning³⁹. Brain specific deletion of *Sirt1* using Nestin-cre decreases monoamine oxidase activity, increases serotonin, and decreases anxiety and depressive-like behavior ^{40,41}. As in the periphery, SIRT1 expression and activity increases in the hypothalamus with fasting to regulate food intake and energy expenditure 42-44. Some of these effects may be mediated by different neuronal populations as deletion of Sirt1 in pro-opiomelanocortin (POMC) neurons decreases energy expenditure and increases susceptibility to diet-induced obesity (DIO) in mice⁴⁵, but deletion of Sirt1 in Agouti-related peptide (AgRP) neurons has the opposite effect and decreases food intake and body weight 46,47. Mice lacking Sirt1 in Sf1 expressing neurons have increased susceptibility to diet-induced obesity and insulin resistance similar to the *Pomc* neuron KO, primarily due to decreased energy expenditure and skeletal muscle insulin sensitivity, but the mice are fertile, and transgenic overexpression prevents these effects⁴⁸. Thus, it appears that Sirt1 may play distinctive and sometimes even opposing roles in energy balance and reproduction

through different neuronal populations. Interpretation of the studies is complicated by the different approaches used to delete the gene. Some studies use deletion of exon 4, which encodes the de-acetylase domain, to create a mutant protein lacking enzyme activity, but other studies delete exons 2-3 that introduces a premature termination codon so no protein is produced. The widespread expression of SIRT1 in both the periphery and CNS makes it difficult to assign a function for SIRT1 in a particular process, therefore we have chosen to create neuron-specific genetic modifications using transgenic cre recombinase that is expressed in a wide range of mature neurons. Using this approach, we recently reported that loss of SIRT1 enzymatic activity in neurons in male mice reduced fasting and glucose-stimulated insulin levels while maintaining normoglycemia suggesting increased insulin sensitivity³⁷. Here we characterized both male and female mice expressing this enzymatically dead SIRT1 mutant, or conversely conditionally overexpressing the wild-type SIRT1 protein, in mature neurons using synapsin-cre to distinguish peripheral from central effects on metabolism and reproduction.

METHODS:

Animals:

Mice having cre recombinase expression under control of the neuron-specific Syntaxin1 promoter (Syn-cre) 49 were mated with mice containing an exon 4 floxed Sirt1 allele or a floxed-STOP Sirt1 allele⁵⁰. Expression of cre deletes exon 4 of SIRT1 that encodes the acetylase domain thus creating a functionally inactive mutant (referred to as N-MUT) from the floxed allele, or causes overexpression of wild-type SIRT1 by deletion of the transcriptional STOP sequence from the flox-STOP allele (referred to as N-OX). The cre driver was maintained on the female side as the *Syn-cre* transgene expresses in the testis⁵¹. Syn-cre mice express the cre transgene as early as e12.5 in differentiated neurons throughout the brain⁴⁹. Homozygous flox/cre- and heterozygous flox/cre- littermates from either the MUT or OX breeding pairs were used as wild-type control (WT). In most experiments no statistical difference was observed between the WT control mice from the N-MUT or N-OX breeding pairs, so the data were combined into a single WT group. Occasionally statistically significant differences were observed between the control groups, in which case the data were analyzed against each separate control groups. Mice were housed in a 12-h light, 12-h dark cycle. Body weights were recorded weekly out to 90 days of age for both genders. Males and females had access to standard chow and water ad libitum. Mouse procedures conformed to the Guide for Care and Use of Laboratory Animals of the US National Institutes of Health and were approved by the Animal Subjects Committee of UCSD.

Caloric Restriction:

At 12 weeks of age, food intake was measured on cohorts of female and male mice for 2 weeks to assess *ad libitum* food intake. For the graded caloric restriction, mice were provided with 90% of prior food intake for week 1, then 80% for week 2, 70% for week 3, then maintained at 60% of original intake for weeks 4-6. Body weight was measured weekly. The study was divided into four phases: before, stage 1 (weeks 1 & 2, 10-20% restriction), stage 2 (weeks 3 & 4, 30-40% restriction), and stage 3 (weeks 5 & 6, 40% restriction). Estrous cycles were monitored in female mice by vaginal cytology for the entire 8 weeks. A cycle was defined as a day of di or metestrus, followed by a day of proestrus, then a day of estrus. The length of the cycle was defined as the number of days between successive days of proestrus in normal DPE cycles

Puberty onset and fertility assessment:

Male and opening MUT, No breeders average

Tissue of Testes, of and RNA for 24 hordewaxed number

Male and female pups were weaned at 21 days of age. Female pups were checked for vaginal opening as a sign of onset of puberty, and monitored for first estrous. For fertility assessment, N-MUT, N-OX or WT female mice were paired on the day of proestrus with known WT male breeders. The number of days to observable vaginal plugs, the number days to the first litter and average number of pups born were recorded.

Tissue collection and histology:

Testes, ovaries, brain, pituitaries and other tissues were harvested at sacrifice for both histology and RNA extraction. Testes were fixed in Bouin's solution for 6 hours and ovaries in formalin for 24 hours followed by washing in 70% ethanol. Paraffin embedded sections (5 μm) were cut, dewaxed, and stained with hematoxylin and eosin. Follicle number and stage, and corpora lutea number were counted on 3-5 sections from ovaries from 4-5 mice per group and are presented as mean number per ovary⁵². Follicle stages were defined as follows: 1° as having a single layer of cuboidal granulosa cells (GCs), 2° as having 2 or more layers of cuboidal GCs but no antrum, early antral as having small patches of clear space between GCs, antral as having clearly defined antrum, atretic as having irregular oocyte morphology. Ovarian sections examined were separated by 50 μm. Images were scanned using Aperio ImageScope and analyzed using the Imagescope software (Leica, Buffalo Grove, IL).

Gene expression:

ADVANCE ARTICLE: JES JOURNAL OF THE ENDOCRINE SOCIETY

Total RNA was extracted from the tissues using RNAbee (Tel-Test Inc. Friendswood, TX) following the manufacturer's instructions. First-strand cDNA was synthesized using a High Capacity cDNA synthesis kit (Applied Biosystems, Waltham, MA). Targeted quantitative PCR (QPCR) assays were run in 20 μL triplicate reactions on a MJ Research Chromo4 instrument using iTaq SYBR Green supermix (Bio-Rad, Hercules, CA). For gene expression assays using 7 nl microfluidic arrays (Fluidigm, San Francisco, CA), mRNA was extracted using RNAbee as before, but it was further purified using RNA purification kits from QIAGEN (Germantown, MD) or Macherey-Nagel (Bethlehem, PA), according to manufacturer's instructions. Custom QPCR primers for a panel of targets were designed and synthesized by Fluidigm for their BioMarkTM HD System. Gene expression levels were calculated after normalization to the housekeeping gene, *m36B4* or *Gapdh* using the 2^{-ΔΔCt} method and expressed as relative mRNA levels compared to the control. Primers are listed in Supplementary Table 1⁵³.

Gonadotropin measurements:

Blood was collected from the tail vein of males and from females at diestrus and proestrus and plasma prepared. Plasma LH and FSH levels were measured by Luminex assay (catalog number RPT86K; Millipore Corp, Bedford, MA). Sensitivity of the assay is as follows LH: 4.9 pg/mL and FSH: 47.7 pg/mL with an intra-assay coefficient of variation of 15%. For the GnRH stimulation test, tail vein blood was collected before and 10 minutes after ip injection of 1 µg/kg GnRH, and gonadotropins were measured.

Intraperitoneal glucose tolerance and insulin tolerance tests:

Mice were subjected to i.p. glucose- and insulin-tolerance tests. Mice were fasted for 6 hours and then injected i.p. with glucose (1 g/kg body weight) or insulin (0.4 U/kg body weight). Tail vein blood glucose was measured at 0, 15, 30, 45, 60, 90, and 120 minutes after injection using a glucose meter (OneTouch Ultra; Bayer Healthcare, Tarrytown, NY). GTT and ITT assays were performed for mice on normal chow and during the last week of 40% food restriction.

Insulin, leptin and steroid measurements:

Animals tail vein Metaboli was as for progester Sensitivi pg/ml; C Metaboli Six mice chamber light and output, reand driph

ADVANCE ARTICLE: JES JOURNAL OF THE ENDOCHINE SOCIETY

Animals were fasted for 6 h. Glucose was measured with a glucose meter, blood drawn from the tail vein and plasma obtained. Fasting insulin and Leptin were measured using the Mouse Metabolic Kit from Meso Scale Discovery, catalog number K15124C-2. Sensitivity of the assay was as follows: Leptin: 43 pg/ml, Insulin: 15 pg/ml; CV 6% and 12% respectively. Estrogen, progesterone and testosterone were measured using a Custom Steroid Hormone Panel Kit (MSD) Sensitivity of the assay was as follows: estradiol 5 pg/ml; progesterone 70 pg/ml; testosterone 20 pg/ml; CV 7%, 15% and 22% respectively.

Metabolic assessment:

Six mice per group (WT and N-OX), matched for body weight, were individually housed in a 12-chamber Clinical Laboratory Animal Monitoring System (CLAMS) with controlled temperature, light and feeding (Columbus Instruments, Columbus, OH). Oxygen uptake, carbon dioxide output, respiratory exchange ratio (RER), horizontal and vertical ambulatory movement, feeding and drinking per 13 minute intervals were measured over a 3-day period. Data from the first 12 h during day 1 acclimation were excluded from the analysis.

Circadian activity:

Female and male mice were raised in a LD 12:12 photoperiod until 3 months of age. Thereafter, mice were singly housed in standard shoebox cages equipped with running wheels (13 cm diameter). Cages were maintained in light-tight secondary enclosures with programmable fluorescent lighting for a three-phase assessment of circadian entrainment and free-running behavior conducted over approximately 6 weeks. Initially, entrained behavior of each mouse was assessed over two weeks in LD 12:12. Thereafter, monitoring continued for an additional two weeks in a skeleton photoperiods consisting of two 1 h light pulses coinciding with the first and last hours of the 12 h light phase. This protocol removes potential masking effects of bright light on locomotor activity. Finally, endogenous circadian rhythmicity was assessed under constant darkness (DD) over 7-10 days. A total of 48 mice were assessed in four cohorts.

Wheel turns were recorded and compiled into 6-min bins. Data were analyzed offline using the Clocklab (Actimetrics; Wilmette, IL) suite of Matlab (Mathworks; Natick, MA) plugins. For each animal, the following variables were calculated in LD and skeleton photoperiods over final 7-day spans of each photoperiod condition. The proper phasing of activity was assessed by calculating the timing of activity onset and offset as defined as the first and last time that the 7-day average activity profile rose above and below the daily mean, respectively. From these data were derived the phase angle of entrainment and the duration of elevated nighttime activity. Disruption of circadian timing was additionally assessed by calculating the proportion of activity intruding into the daytime (central 8 h of the light phase or skeleton daytime). Rhythm robustness was assessed by calculating the maximum amplitude of the chi-square periodogram. In the first 7 days of DD, free-running period was estimated a) as the value with the highest amplitude in the chi-square periodogram and b) the best-fit linear regression line through identified activity onsets. These methods yielded comparable estimates and only the former is reported here. Individually identified activity onsets were additionally used to determine the cycle-to-cycle variability in free-running activity onset. In all phases, total amount of wheel-running activity without respect to its timing was also assessed. All data were analyzed with 4-way ANOVA with cohort, strain (OX vs MUT), Cre genotype (Cre+ or Cre-) and sex (M or F) as between subjects factors. For phenotype screening, alpha was set initially at 0.05 without correction for multiple comparisons.

Statistical analysis:

Data were analyzed by ANOVA or Students t-test as appropriate using Graph Pad Prism (GraphPad, La Jolla, CA) or in R. Pairwise comparisons were performed using Tukey *post hoc* tests following the ANOVA. Results were expressed as Mean+/-Standard Error and considered significant with p<0.05. Supplementary data is available online. ⁵³

RESULTS:

Overexpression of SIRT1 in neurons caused glucose intolerance.

To test the role of neuronal SIRT1 in metabolic and reproductive regulation, we generated mice expressing an enzymatically inactive form of SIRT1 (N-MUT) ³⁷ or overexpressing wild-type SIRT1 (N-OX) in neurons. Assessment of Sirt1 mRNA expression in whole brains from N-OX mice indicated that the gene is overexpressed approximately 2.5-fold (Supplementary Figure S1A⁵³). The body weights of male mice indicated a significant difference with genotype over the first 3 months although no significant difference was observed at 8-9 months of age (Fig. 1A), and the female mice did not differ appreciably in body weight (Fig. 1B). Food intake did not differ in male mice, but the female N-MUT mice ate significantly more (Fig. 1G and H) despite having equivalent body weight. The male N-OX mice were significantly glucose intolerant (Fig. 1C) unlike the N-MUT mice as we have previously published. Consistent with the male mice, the female N-OX mice also showed glucose intolerance, but the N-MUT mice showed significantly improved glucose tolerance compared to WT controls (Fig. 1D). Neither the N-MUT nor N-OX groups showed altered insulin tolerance in male mice, but the female N-MUT mice were significantly more insulin sensitive than WT or N-OX littermates (Fig. 1E and F). Fasting blood glucose and insulin levels and homeostatic model of assessment of insulin resistance (HOMA-IR) were comparable between the groups and sexes (Fig. 1I to L, Supplementary Figure S1B⁵³) but leptin levels were significantly lower in N-OX mice for both sexes (Fig. 1M and N).

Overexpression of SIRT1 impaired estrous cycles.

Neither N-MUT nor N-OX female mice differed in the day of vaginal opening (Fig. 2A) but the N-OX mice reached first estrous slightly earlier (Fig. 2B), indicating that all genotypes went through puberty normally. Assessment of the number of estrous cycles over 6 weeks after the onset of estrous cycles showed that N-OX mice had fewer cycles (Fig. 2C), and analysis of cycle length indicated that N-OX mice tended to have a slightly longer mean cycle length (Fig. 2D, 6.6 days for N-MUT, 6.5 days for WT, and 7.8 days for N-OX) with more extended cycles (Fig. 2E). The N-OX mice had significantly more days of estrus and fewer days of diestrus (Fig. 2F). Representative cyclegrams are given in Supplementary Figure 2⁵³. No differences in follicle stimulating hormone (FSH) were observed in N-OX mice at diestrus, the morning or evening of proestrus, or on estrus, but the WT mice showed the expected higher levels during late proestrus and estrus (Fig. 2G). Luteinizing hormone (LH) levels were elevated at diestrus in N-MUT mice but no differences were observed in early proestrus or on estrus (Fig. 2H). LH levels during late proestrus showed LH surges in N-MUT (2/8) and WT (8/16) mice but no surges were observed in N-OX mice (Fig. 2I). Measurement of progesterone levels confirmed that N-OX mice had not ovulated compared to WT mice (Fig. 2J). These results suggested that spontaneous LH surges might be impaired in the N-OX mice, so we tested fertility directly by pairing female mice on proestrus with known male WT breeders. The number of days until the observation of vaginal plugs, the number of days until first litter and the litter size did not show a difference with genotype (Fig. 1K), indicating the mice were fertile and could ovulate given normal environmental cues. Comparison of ovarian histology (Fig. 3A) showed that N-OX ovaries were

smaller (Fig. 3B) and did not show a difference in follicle development (Fig. 3C), but corpora lutea were significantly reduced in the N-OX mice consistent with the decreased LH surges and progesterone levels (Fig. 3D). Male mice were not studied reproductively as the synapsin-cre expresses in the testis⁵¹.

Mice overexpressing SIRT1 in neurons were more sensitive to improvements in glucose tolerance and estrous cycle arrest due to caloric restriction.

We then tested whether neuronal SIRT1 might alter the response to caloric restriction (CR). To avoid the induction of an adrenal stress response due to a rapid reduction in food intake, we used a gradual reduction of food intake over four weeks, 10% per week, then maintained the mice for a further 2 weeks at 40% caloric restriction. Assessment of glucose tolerance during the last week showed that the N-OX mice had improved glucose tolerance (Fig. 4A). Insulin levels were higher in WT and N-OX mice during the initial stage of CR consistent with fasting-induced insulin-resistance, but then returned to normal (Fig. 4B). In contrast, leptin levels decreased progressively during CR (Fig. 4C) and the N-OX mice showed consistently lower leptin levels as we had seen earlier (Fig. 1M and N).

Estrous cycles were assessed in the female mice during the entire period of caloric restriction. N-MUT mice showed the same response as WT mice with a gradual increase in the days of diestrus and a decrease in the days at proestrus and estrus (Fig. 5A). In contrast, the N-OX mice had fewer days at diestrus before CR, did not respond to the 10-20% restriction, but showed a steep increase in the days of diestrus during the 30-40% restriction such that all mice were in permanent diestrus by 40% CR. This was confirmed by determining the relative frequency of diestrus arrest at each CR stage for each genotype (Supplementary Figure S3A⁵³). The WT and N-MUT mice had the highest frequency of arrest at 40% CR but the N-OX mice had the highest frequency of arrest at 20-30% CR. Unexpectedly, we did not observe a significant decrease in LH during CR in any genotype (Fig. 5B), but we did observed an increase in FSH even at the lowest level of CR (Fig. 5C). Interestingly, this response was sexually dimorphic as FSH levels decreased in male mice on CR, but LH levels did not change (Supplementary Figure S3B⁵³). Inspection of ovarian histology at sacrifice showed that all mice had ceased cycling as no corpora lutea were observed (Supplementary Figure S4⁵³). Steroid hormone levels were measured at sacrifice. Estrogen levels were slightly higher with CR but were significantly lower in WT mice than N-MUT and N-OX mice (Fig. 5D). Progesterone levels increased during CR (Fig. 5E) and testosterone levels showed an increase with CR but also a genotype effect with N-MUT mice having significantly higher levels of testosterone (Fig. 5F).

Altered hypothalamic gene expression in mice on caloric restriction.

RNA was extracted from hypothalami and pituitaries from female mice sacrificed at the end of CR. The N-OX mice showed approximately 2-fold overexpression of *Sirt1* by QPCR (Fig. 6A) as observed before (Fig. 1). The neuropeptide Y (*Npy*), pro-opiomelanocortin (*Pomc*) and agouti-related peptide genes (*Agrp*) that control food intake and energy expenditure were increased in the N-OX mice, but the cocaine and amphetamine-regulated transcript (*Cart*) was unchanged (Fig. 6A). The reproductive neuropeptides gonadotropin-releasing hormone 1 (*Gnrh1*), and the RF-amide related peptide 3 (RFRP3, GnIH) precursor gene (*Npvf*) were significantly altered but the kisspeptin gene (*Kiss1*) was unchanged (Fig. 6A). Neuropeptide receptor gene expression did not change with genotype (Supplementary Figure S3C⁵³). The same alterations in hypothalamic gene expression were not seen in male mice (Supplementary Figure S5⁵³). Assessment of pituitary gene expression in female mice indicated a 3-fold increase in *Fshb* gene expression in N-OX mice, an increase in the glycoprotein hormone alpha gene

(Cga) in the N-MUT mice, and decreases in growth hormone (Gh) and pituitary adenylate-cyclase activating peptide (Adcyap1) gene expression in N-MUT mice (Fig. 6B).

Mice overexpressing SIRT1 showed altered activity during the dark phase.

As the N-OX mice were glucose intolerant, we subjected N-OX and WT mice to a metabolic assessment with continuous monitoring over 3 days. The N-OX mice showed stronger diurnal changes in ambulatory and rearing activity (Fig. 7A & B). The onset of activity at the start of the dark phase was similar but the N-OX mice showed greater activity and sustained that activity throughout the entire dark phase whereas the WT mice reduced activity in anticipation of the light phase. The difference in average activity between the dark and light phase was also increased (Supplementary Figure S6⁵³). There was no significant difference in body weight between genotypes at the end of the assessment. Oxygen consumption was also altered with lower consumption at the start of dark phase but higher consumption at the end of the dark phase (Fig. 7C) and the respiratory exchange ratio showed a genotype effect with greater lipid oxidative metabolism during the light phase in the N-OX mice consistent with greater fasting (Fig. 7D). Food intake showed a diurnal variation but no genotype effect, whereas water intake showed a weak genotype effect (Fig. 7E & F). Heat production and cage temperature showed the expected diurnal variation but no genotype effect (Fig. 7G & H).

Mice lacking or overexpressing SIRT1 in neurons did not show altered circadian activity. SIRT1 has been implicated in the regulation of the central circadian clock via de-acetylation of PGC-1α. ⁵⁴ Therefore we initially assessed activity during regular 12h/12h light/dark (LD) cycles, then 2h/22h skeleton periods, then 24h continual darkness (DD). In LD, female mice showed more robust rhythms (p<0.05) than male mice (Supplementary Table 2⁵³) and showed higher total activity counts and average counts (p<0.001). Mice initiated wheel-running shortly after lights off according to the expected nocturnal pattern, and showed the same period and activity onset and offset. The sex difference in rhythm robustness, average counts and total counts persisted in the skeleton photoperiods (p<0.05, 0.01 and 0.01 respectively). There were small genotype differences in rhythm robustness, 8h daytime counts, activity onset, and activity period but none reached significance. In DD, the period showed a strain effect (p<0.05) with all MUT strain mice having slightly shorter period, and rhythm robustness showed a genotype effect (p<0.05) with the MUT genotype having greater robustness. In summary, SIRT1 overexpressing and mutant mice generated species-typical circadian locomotor activity rhythms, with the major difference being female mice showed greater activity and more robust rhythms.

DISCUSSION

Previously, loss of SIRT1 enzyme activity in neurons did not alter glucose metabolism in male mice but increased insulin sensitivity in the brain and periphery, and partially protected mice from high-fat diet induced obesity³⁷. Here we studied the same neuronal SIRT1 mutant lacking enzyme activity (N-MUT), but also studied the effect of overexpression of wild-type SIRT1 (N-OX) in neurons. In male mice we observed that the N-MUT did not alter glucose tolerance as before, but we did observe decreased glucose tolerance with overexpression of SIRT1 (N-OX), which is consistent with the previous report on the N-MUT mice. In contrast, female mice showed an improvement in glucose tolerance in the N-MUT transgenic mouse, and an impairment in the N-OX overexpressing mouse. Unlike the male mice, the female N-MUT mice showed a slight increase in insulin sensitivity by ITT but fasting blood glucose and insulin were not changed, and consequently HOMA-IR was not significantly different. As SIRT1 has been

implicated in the response to food restriction, the mice were challenged with a gradual but progressive caloric restriction down to 60% of their normal food intake over 6 weeks. All mice, male and female showed improved glucose tolerance, and the N-OX mice showed better glucose tolerance than their littermates after CR, instead of worse glucose tolerance as had been seen for mice on *ad libitum* normal chow. This suggested that the overexpression of SIRT1 rendered the mice more sensitive to the metabolic effects of caloric restriction.

In a previous study, deletion of SIRT1 enzyme activity (Δ exon 4) in neurons, astrocytes, glia and the pituitary using nestin-cre disrupts the GH-IGF1 axis causing runting⁴³. Young mice displayed normal glucose tolerance but older mice were glucose intolerant. Caloric restriction improved glucose tolerance in both wild-type and the total brain KO mice indicating that SIRT1 enzyme activity was not required for the metabolic response to CR⁴³. These KO mice showed increased physical activity in a wheel-running experiment but did not subsequently respond to CR. A subsequent study showed that this activity difference correlated with lower anxiety and increased exploratory drive due to decreased monoamine oxidase activity and increased serotonin and norepinephrine levels⁴¹. These studies are confounded however by the observation that SIRT1 is essential for neural fate determination in neural stem cells and could alter the final balance of neuronal, astrocyte and oligodendrocyte populations, including Npy/AgRP and Pomc neurons⁵⁵⁻⁵⁸. More focused deletion in specific neuronal populations has produced conflicting results. Deletion of Sirt1 in either *Pomc* or *Sf1* neurons decreases energy expenditure and increases susceptibility to diet-induced obesity but has no effect for mice on normal chow 45,48. but deletion in Agrp neurons has the opposite effect and decreases food intake and body weight^{46,47}. Transgenic SIRT1 overexpression in *Pomc* or *Sf1* neurons increased energy expenditure, increased insulin sensitivity and reduced body weight. The opposite effect was observed when Sirt1 was overexpressed in the mouse forebrain using the CMKIIα promoter, which caused decreased energy expenditure, decreased physical activity, obesity and glucose intolerance⁵⁹. We did not see an effect on body weight in either the female N-OX or N-MUT mice on normal chow, similar to the Pomc or Sf1 neuron knockouts, but we observed an increase in physical activity and VO₂ in female N-OX, and our mice were glucose intolerant. In addition, overexpression of SIRT1 using the mouse prion *Prp* promoter caused an enhanced response to caloric restriction as measured by physical activity counts⁴⁴ in agreement with our study. This confirms the ability of SIRT1 to mediate the central metabolic effects of CR but overexpression of SIRT1 alone may not be sufficient to mimic CR.

At the reproductive level, complete loss of *Sirt1* results in hypogonadotropic hypogonadism due to failure of *Gnrh* neurons to migrate²⁸. Female pubertal development was normal in the N-OX and N-MUT mice. Overexpression of SIRT1 impaired estrous cycles, and increased the number of days in estrus, perhaps because the N-OX mice did not show the normal increase in FSH during estrus to start the next follicular cycle. LH and progesterone surges were absent on the evening of proestrus in the N-OX mice consistent with a defect in ovulation, which was confirmed by the ovarian histology that showed a reduced number of corpora lutea. This agrees with a study reporting that the SIRT1 activator SRT1720 reduced ovary size and reduced the number of corpora lutea⁶⁰. Despite these defects, the mice were still fertile when mated to wild-type mice on the day of pro-estrus indicating that the mice can respond to normal pheromonal or environmental cues. When subjected to CR, the N-OX mice went into diestrus arrest earlier than their littermates suggesting that the overexpression of SIRT1 also renders mice more sensitive to the suppression of reproductive cycles. Unlike other fasting studies, LH levels did not decrease with the gradual CR indicating that we avoided an adrenal stress response which is known to

suppress LH. We noticed a consistent increase in plasma FSH during CR in female, but not male, mice independent of genotype. It is possible that this increase with CR allows the N-OX mice to leave estrus and reenter the estrous cycle before arresting in the next diestrus. The origin of this increase in FSH is not known but we observed a significant increase in pituitary *Fshb* mRNA in the N-OX mice with CR. Interestingly, loss of SIRT1 has been implicated in increased *Fshb* production by pituitary gonadotropes⁶¹. We also observed increases in hypothalamic *Npy* and *Agrp* mRNAs in the N-OX mice on CR, which may underlie the effects of caloric restriction as they inhibit GnRH neurons to suppress reproductive cycles.

Lastly, SIRT1 has also been implicated in circadian rhythms in the suprachiasmatic nucleus⁵⁴ and in relaying nutritional inputs to the clock via Sf1 neurons in the VMH⁶². The total brain SIRT1 knockout has increased photoperiod, and the SIRT1 overexpressors have decreased photoperiod compared to WT controls⁵⁴. In our study, neither N-OX nor N-MUT mice demonstrated a circadian phenotype but it is possible that the synapsin-cre does not express in SCN neurons although synapsin 1 is a reliable marker for synapse formation in the SCN⁶³. Further studies will be needed to resolve this discrepancy.

National Cancer Institute http://dx.doi.org/10.13039/100000054, CA196853, Nicholas Webster; National Institute of Child Health and Human Development http://dx.doi.org/10.13039/100000071, HD012303, Nicholas Webster; U.S. Department of Veterans Affairs http://dx.doi.org/10.13039/100000738, I01BX000130, Nicholas Webster; National Cancer Institute http://dx.doi.org/10.13039/100000054, CA023100, Not Applicable

Acknowledgements.

We would like to acknowledge the assistance of the Histology Core at the Moores' Cancer Center (supported by NIH CA023100), and the Genomics Core at the Sanford Consortium for Regenerative Medicine. This work is funded in part by NIH grants to N.J.G.W. (HD012303, CA155435, CA196853) and a VA Merit Review award to N.J.G.W. (I01BX000130).

Corresponding author: Nicholas Webster, PhD, Department of Medicine – 0673, University of California, San Diego, 9500 Gilman Drive, La Jolla, CA 92093, Email: nwebster@ucsd.edu

DISCLOSURE STATEMENT:

The authors have nothing to disclose.

References

- 1. Haigis MC, Sinclair DA. Mammalian sirtuins: biological insights and disease relevance. *Annu Rev Pathol.* 2010;5:253-295.
- 2. McBurney MW, Clark-Knowles KV, Caron AZ, Gray DA. SIRT1 is a Highly Networked Protein That Mediates the Adaptation to Chronic Physiological Stress. *Genes Cancer*. 2013;4(3-4):125-134.
- 3. Chang HC, Guarente L. SIRT1 and other sirtuins in metabolism. *Trends Endocrinol Metab.* 2014;25(3):138-145.
- 4. Boutant M, Canto C. SIRT1 metabolic actions: Integrating recent advances from mouse models. *Mol Metab.* 2014;3(1):5-18.
- 5. Chalkiadaki A, Guarente L. High-fat diet triggers inflammation-induced cleavage of SIRT1 in adipose tissue to promote metabolic dysfunction. *Cell Metab.* 2012;16(2):180-188.

- 6. Seyssel K, Alligier M, Meugnier E, et al. Regulation of energy metabolism and mitochondrial function in skeletal muscle during lipid overfeeding in healthy men. *J Clin Endocrinol Metab.* 2014;99(7):E1254-1262.
 7. Lomb DJ, Laurent G, Haigis MC. Sirtuins regulate key aspects of lipid metabolism. *Biochim Biophys Acta.* 2010;1804(8):1652-1657.
- 8. Heyward FD, Walton RG, Carle MS, Coleman MA, Garvey WT, Sweatt JD. Adult mice maintained on a high-fat diet exhibit object location memory deficits and reduced hippocampal SIRT1 gene expression. *Neurobiol Learn Mem.* 2012;98(1):25-32.
- 9. Qiang L, Wang L, Kon N, et al. Brown remodeling of white adipose tissue by SirT1-dependent deacetylation of Ppargamma. *Cell.* 2012;150(3):620-632.
- 10. Pfluger PT, Herranz D, Velasco-Miguel S, Serrano M, Tschop MH. Sirt1 protects against high-fat diet-induced metabolic damage. *Proc Natl Acad Sci U S A*. 2008;105(28):9793-9798.
- 11. Boutant M, Joffraud M, Kulkarni SS, et al. SIRT1 enhances glucose tolerance by potentiating brown adipose tissue function. *Mol Metab.* 2015;4(2):118-131.
- 12. Wang RH, Sengupta K, Li C, et al. Impaired DNA damage response, genome instability, and tumorigenesis in SIRT1 mutant mice. *Cancer Cell.* 2008;14(4):312-323.
- 13. Cheng HL, Mostoslavsky R, Saito S, et al. Developmental defects and p53 hyperacetylation in Sir2 homolog (SIRT1)-deficient mice. *Proceedings of the National Academy of Sciences of the United States of America*. 2003;100(19):10794-10799.
- 14. McBurney MW, Yang X, Jardine K, et al. The mammalian SIR2alpha protein has a role in embryogenesis and gametogenesis. *Mol Cell Biol.* 2003;23(1):38-54.
- 15. Xu F, Gao Z, Zhang J, et al. Lack of SIRT1 (Mammalian Sirtuin 1) activity leads to liver steatosis in the SIRT1+/- mice: a role of lipid mobilization and inflammation. *Endocrinology*. 2010;151(6):2504-2514.
- 16. Ding RB, Bao J, Deng CX. Emerging roles of SIRT1 in fatty liver diseases. *Int J Biol Sci.* 2017;13(7):852-867.
- 17. Seifert EL, Caron AZ, Morin K, et al. SirT1 catalytic activity is required for male fertility and metabolic homeostasis in mice. *Faseb J.* 2012;26(2):555-566.
- 18. Caron AZ, He X, Mottawea W, et al. The SIRT1 deacetylase protects mice against the symptoms of metabolic syndrome. *Faseb J.* 2014;28(3):1306-1316.
- 19. Gillum MP, Kotas ME, Erion DM, et al. SirT1 regulates adipose tissue inflammation. *Diabetes*. 2011;60(12):3235-3245.
- 20. Schenk S, McCurdy CE, Philp A, et al. Sirt1 enhances skeletal muscle insulin sensitivity in mice during caloric restriction. *J Clin Invest*. 2011;121(11):4281-4288.
- 21. Wang RH, Li C, Deng CX. Liver steatosis and increased ChREBP expression in mice carrying a liver specific SIRT1 null mutation under a normal feeding condition. *International journal of biological sciences*. 2010;6(7):682-690.
- 22. Li Y, Wong K, Giles A, et al. Hepatic SIRT1 Attenuates Hepatic Steatosis and Controls Energy Balance in Mice by Inducing Fibroblast Growth Factor 21. *Gastroenterology*. 2014;146(2):539-549 e537.
- 23. Purushotham A, Schug TT, Xu Q, Surapureddi S, Guo X, Li X. Hepatocyte-specific deletion of SIRT1 alters fatty acid metabolism and results in hepatic steatosis and inflammation. *Cell Metab.* 2009;9(4):327-338.
- 24. Bordone L, Cohen D, Robinson A, et al. SIRT1 transgenic mice show phenotypes resembling calorie restriction. *Aging Cell.* 2007;6(6):759-767.

- 25. Boutant M, Kulkarni SS, Joffraud M, et al. SIRT1 Gain of Function Does Not Mimic or Enhance the Adaptations to Intermittent Fasting. *Cell Rep.* 2016;14(9):2068-2075.
- 26. Boutant M, Canto C. SIRT1: A novel guardian of brown fat against metabolic damage. *Obesity (Silver Spring)*. 2016;24(3):554.
- 27. Li H, Rajendran GK, Liu N, Ware C, Rubin BP, Gu Y. SirT1 modulates the estrogen-insulin-like growth factor-1 signaling for postnatal development of mammary gland in mice. *Breast Cancer Res.* 2007;9(1):R1.
- 28. Di Sante G, Wang L, Wang C, et al. Sirt1-deficient mice have hypogonadotropic hypogonadism due to defective GnRH neuronal migration. *Mol Endocrinol.* 2015;29(2):200-212.
- 29. Bell EL, Nagamori I, Williams EO, et al. SirT1 is required in the male germ cell for differentiation and fecundity in mice. *Development*. 2014;141(18):3495-3504.
- 30. Kolthur-Seetharam U, Teerds K, de Rooij DG, et al. The histone deacetylase SIRT1 controls male fertility in mice through regulation of hypothalamic-pituitary gonadotropin signaling. *Biol Reprod.* 2009;80(2):384-391.
- 31. Tatone C, Di Emidio G, Vitti M, et al. Sirtuin Functions in Female Fertility: Possible Role in Oxidative Stress and Aging. *Oxid Med Cell Longev*. 2015;2015:659687.
- 32. Dai Y, Ngo D, Forman LW, Qin DC, Jacob J, Faller DV. Sirtuin 1 is required for antagonist-induced transcriptional repression of androgen-responsive genes by the androgen receptor. *Mol Endocrinol*. 2007;21(8):1807-1821.
- 33. Fu M, Liu M, Sauve AA, et al. Hormonal control of androgen receptor function through SIRT1. *Mol Cell Biol.* 2006;26(21):8122-8135.
- 34. Montie HL, Pestell RG, Merry DE. SIRT1 modulates aggregation and toxicity through deacetylation of the androgen receptor in cell models of SBMA. *J Neurosci.* 2011;31(48):17425-17436.
- 35. Moore RL, Faller DV. SIRT1 represses estrogen-signaling, ligand-independent ERalphamediated transcription, and cell proliferation in estrogen-responsive breast cells. *J Endocrinol*. 2013;216(3):273-285.
- 36. Herskovits AZ, Guarente L. SIRT1 in neurodevelopment and brain senescence. *Neuron*. 2014;81(3):471-483.
- 37. Lu M, Sarruf DA, Li P, et al. Neuronal Sirt1 deficiency increases insulin sensitivity in both brain and peripheral tissues. *J Biol Chem.* 2013;288(15):10722-10735.
- 38. Albani D, Polito L, Forloni G. Sirtuins as novel targets for Alzheimer's disease and other neurodegenerative disorders: experimental and genetic evidence. *J Alzheimers Dis*. 2010;19(1):11-26.
- 39. Michan S, Li Y, Chou MM, et al. SIRT1 is essential for normal cognitive function and synaptic plasticity. *J Neurosci.* 2010;30(29):9695-9707.
- 40. Abe-Higuchi N, Uchida S, Yamagata H, et al. Hippocampal Sirtuin 1 Signaling Mediates Depression-like Behavior. *Biol Psychiatry*. 2016;80(11):815-826.
- 41. Libert S, Pointer K, Bell EL, et al. SIRT1 activates MAO-A in the brain to mediate anxiety and exploratory drive. *Cell.* 2011;147(7):1459-1472.
- 42. Boily G, Seifert EL, Bevilacqua L, et al. SirT1 regulates energy metabolism and response to caloric restriction in mice. *PLoS One*. 2008;3(3):e1759.
- 43. Cohen DE, Supinski AM, Bonkowski MS, Donmez G, Guarente LP. Neuronal SIRT1 regulates endocrine and behavioral responses to calorie restriction. *Genes Dev.* 2009;23(24):2812-2817.

- 44. Satoh A, Brace CS, Ben-Josef G, et al. SIRT1 promotes the central adaptive response to diet restriction through activation of the dorsomedial and lateral nuclei of the hypothalamus. *The Journal of neuroscience : the official journal of the Society for Neuroscience*. 2010;30(30):10220-10232.
- 45. Ramadori G, Fujikawa T, Fukuda M, et al. SIRT1 deacetylase in POMC neurons is required for homeostatic defenses against diet-induced obesity. *Cell Metab.* 2010;12(1):78-87.
- 46. Dietrich MO, Antunes C, Geliang G, et al. Agrp neurons mediate Sirt1's action on the melanocortin system and energy balance: roles for Sirt1 in neuronal firing and synaptic plasticity. *The Journal of neuroscience : the official journal of the Society for Neuroscience*. 2010;30(35):11815-11825.
- 47. Sasaki T, Kikuchi O, Shimpuku M, et al. Hypothalamic SIRT1 prevents age-associated weight gain by improving leptin sensitivity in mice. *Diabetologia*. 2014;57(4):819-831.
- 48. Ramadori G, Fujikawa T, Anderson J, et al. SIRT1 deacetylase in SF1 neurons protects against metabolic imbalance. *Cell Metab.* 2011;14(3):301-312.
- 49. Zhu Y, Romero MI, Ghosh P, et al. Ablation of NF1 function in neurons induces abnormal development of cerebral cortex and reactive gliosis in the brain. *Genes Dev.* 2001;15(7):859-876.
- 50. Oberdoerffer P, Michan S, McVay M, et al. SIRT1 redistribution on chromatin promotes genomic stability but alters gene expression during aging. *Cell.* 2008;135(5):907-918.
- 51. Rempe D, Vangeison G, Hamilton J, Li Y, Jepson M, Federoff HJ. Synapsin I Cre transgene expression in male mice produces germline recombination in progeny. *Genesis*. 2006;44(1):44-49.
- 52. Myers M, Britt KL, Wreford NG, Ebling FJ, Kerr JB. Methods for quantifying follicular numbers within the mouse ovary. *Reproduction*. 2004;127(5):569-580.
- 53. Rickert E, Fernandez M, Choi I, Gorman M, Olefsky J, Webster N. Rickert-2018-Supplementary-Data 2018. https://doi.org/10.6084/m9.figshare.7396940.v1.
- 54. Chang HC, Guarente L. SIRT1 mediates central circadian control in the SCN by a mechanism that decays with aging. *Cell.* 2013;153(7):1448-1460.
- 55. Cai Y, Xu L, Xu H, Fan X. SIRT1 and Neural Cell Fate Determination. *Mol Neurobiol*. 2016;53(5):2815-2825.
- 56. Desai M, Li T, Han G, Ross MG. Programmed hyperphagia secondary to increased hypothalamic SIRT1. *Brain Res.* 2014;1589:26-36.
- 57. Rafalski VA, Ho PP, Brett JO, et al. Expansion of oligodendrocyte progenitor cells following SIRT1 inactivation in the adult brain. *Nat Cell Biol.* 2013;15(6):614-624.
- 58. Saharan S, Jhaveri DJ, Bartlett PF. SIRT1 regulates the neurogenic potential of neural precursors in the adult subventricular zone and hippocampus. *J Neurosci Res.* 2013;91(5):642-659.
- 59. Wu D, Qiu Y, Gao X, Yuan XB, Zhai Q. Overexpression of SIRT1 in mouse forebrain impairs lipid/glucose metabolism and motor function. *PLoS One*. 2011;6(6):e21759.
- 60. Zhou XL, Xu JJ, Ni YH, et al. SIRT1 activator (SRT1720) improves the follicle reserve and prolongs the ovarian lifespan of diet-induced obesity in female mice via activating SIRT1 and suppressing mTOR signaling. *J Ovarian Res.* 2014;7:97.
- 61. Lannes J, L'Hote D, Garrel G, Laverriere JN, Cohen-Tannoudji J, Querat B. Rapid communication: A microRNA-132/212 pathway mediates GnRH activation of FSH expression. *Mol Endocrinol.* 2015;29(3):364-372.

- 62. Orozco-Solis R, Ramadori G, Coppari R, Sassone-Corsi P. SIRT1 Relays Nutritional Inputs to the Circadian Clock Through the Sf1 Neurons of the Ventromedial Hypothalamus. *Endocrinology*. 2015;156(6):2174-2184.
- 63. Moore RY, Bernstein ME. Synaptogenesis in the rat suprachiasmatic nucleus demonstrated by electron microscopy and synapsin I immunoreactivity. *J Neurosci*. 1989;9(6):2151-2162.

Figure 1: Neuronal SIRT1 causes glucose intolerance. For all figures N-MUT mice are shown in red, wild-type littermates in white, and N-OX mice in green. A. Body weights for male mice from 3 weeks to 13 weeks of age (n=13 for N-MUT, n=48 for WT, n=24 for N-OX). 2-way ANOVA indicates significant genotype and time effects (p<0.0001) but no interaction. Inset shows final body weight at 8-9 months. **B.** Body weights for female mice from 3 weeks to 13 weeks of age (n=10 for N-MUT, n=44 for WT, n=20 for N-OX). 2-way ANOVA indicates significant genotype and time effects (p<0.0001) but no interaction. Inset shows final body weight at 8-9 months. C. Glucose tolerance test performed in male mice at 3 months of age (n=8) for N-OX, n=16 for WT, n=4 for N-MUT). 2-way ANOVA indicates significant genotype and time effects (p<0.0001) and interaction (p=0.005). Inset shows area under the curve. **D.** Glucose tolerance test performed in female mice at 3 months of age (n=9 for N-OX, n=16 for WT, n=6 for N-MUT). 2-way ANOVA indicates significant genotype and time effects (p<0.0001) but no interaction. Inset shows area under the curve. E. Insulin tolerance test performed in male mice at 3 months of age (n=9 for N-OX, n=16 for WT, n=6 for N-MUT). 2-way ANOVA indicates significant genotype and time effects (p<0.01 and p<0.0001) but no interaction. **F.** Insulin tolerance test performed in female mice at 3 months of age (n=10 for N-OX, n=16 for WT, n=6 for N-MUT). 2-way ANOVA indicates significant genotype and time effects (p<0.001 and p<0.0001) but no interaction. G. Daily food intake over 10 weeks for male mice (n=3 for N-MUT, n=12 for WT, n=4 for N-OX). **H.** Daily food intake over 10 weeks for female mice (n=6 for N-MUT, n=11 for WT, n=5 for N-OX). I. Fasting blood glucose in male mice (n=17 for N-OX, n=32 for WT, n=8 for N-MUT). J. Fasting blood glucose in female mice (n=20 for N-OX n=32 for WT, n=4 for N-MUT). **K.** Fasting insulin in male mice (n=6 for N-MUT, n=14 for WT, n=6 for N-OX). L. Fasting insulin in female mice (n=6 for N-MUT, n=12 for WT, n=6 for N-OX). M. Fasting leptin in male mice (n=6 for N-MUT, n=14 for WT, n=6 for N-OX). N. Fasting leptin in female mice (n=6 for N-MUT, n=12 for WT, n=6 for N-OX). Data shown are mean ± SEM. Asterisks report significance vs WT or as indicated; *p<0.05, **p<0.01, *p<0.001, ****p<0.0001.

Figure 2: Neuronal SIRT1 regulates reproduction in female mice. Color scheme is same as Figure 1. **A.** Day of vaginal opening (n=8 for N-MUT, n=40 for WT, n=18 for N-OX). **B.** Day of first estrous (n=8 for N-MUT, n=41 for WT, n=21 for N-OX). **C.** Number of estrous cycles by vaginal lavage over 6 weeks (n=6 for N-MUT, n=11 for WT, n=5 for N-OX). **D.** Cycle length during the 6 weeks (n=44 for N-MUT, n=74 for WT, n=19 for N-OX). **E.** Relative frequency histogram of cycle lengths. **F.** Percentage of days spent in each stage of the estrous cycle during the 6-week cycling (n=6 for N-MUT, n=11 for WT, n=5 for N-OX). 2-way ANOVA indicates significant stage effect (p<0.0001) and significant interaction of stage and genotype (p<0.0001). **G.** FSH levels during diestrus, the morning of pro-estrus, the afternoon of proestrus, and the morning of estrus (n=8 for N-MUT, n=16 for WT, n=8 for N-OX). 2-way ANOVA indicates significant stage effect (p=0.015) and significant interaction of stage and genotype (p=0.013). **H.** LH levels during diestrus, the morning of pro-estrus, and the morning of estrus (n=8 for N-MUT,

n=16 for WT, n=8 for N-OX). 2-way ANOVA indicates significant stage effect (p=0.013) but no interaction of stage and genotype. **I.** LH levels during the afternoon of proestrus (n=8 for N-MUT, n=16 for WT, n=8 for N-OX). Proestrus LH values do not follow a normal distribution, so N-OX mice have significantly lower LH than WT mice by Kruskal-Wallis test (p=0.033). **J.** Progesterone levels during the afternoon of proestrus (n=7 for WT, n=7 for N-OX). **K.** Days to plug, days to first litter and litter size during fertility test (n=3 for N-MUT, n=11 for WT, n=6 for N-OX). Data shown are mean ± SEM. Asterisks report significance vs WT or as indicated; *p<0.05, **p<0.01, *p<0.001, ****p<0.0001.

Figure 3: Overexpression of SIRT1 impairs ovulation. Color scheme is same as Figure 1. **A.** Ovarian morphology. Representative H&E stained sections of ovaries obtained at sacrifice. AF indicates antral follicle, CL indicates corpora lutea. B. Quantification of ovarian cross-sectional area for N-MUT (n=12), WT (n=15) and N-OX (n=8) ovaries. *p<0.05 v.s. N-MUT. **C.** Quantification of follicle stage. Percentage of follicles at each stage for N-MUT (n=6), WT (n=9) and N-OX (n=4) mice. **D.** Quantification of corpora lutea for N-MUT (n=6), WT (n=9) and N-OX (n=4) mice. *p<0.05 v.s. WT. Data are shown as mean ±SEM. Asterisks indicate significance by post-hoc testing.

Figure 4: Overexpression of SIRT1 enhances the metabolic response to caloric restriction. Color scheme is same as Figure 1. **A.** Glucose tolerance test performed after caloric restriction (n=8 for N-OX, n=17 for WT, n=6 for N-MUT, n=20 males, n=11 females). 2-way ANOVA indicates significant time effect (p<0.0001) and time-genotype interaction (p=0.0025). **B.** Fasting insulin during CR (n=14 for N-MUT, n=26 for WT, n=12 for N-OX, n=28 males, n=24 females). **C.** Fasting leptin during CR (n=14 for N-MUT, n=26 for WT, n=12 for N-OX, n=28 males, n=24 females). 2-way ANOVA indicates significant genotype effect (p<0.0001). Data are shown as mean ± SEM. Asterisks indicate significant differences between N-OX and WT and N-MUT, or as indicated, from post-hoc testing; *p<0.05, **p<0.01.

Figure 5: Overexpression of SIRT1 enhances the reproductive response to caloric **restriction.** Color scheme is same as Figure 1. Estrous cycles were assessed by vaginal lavage in female mice during the eight weeks of caloric restriction. Data are shown as mean \pm SEM. A. Average number of days spent in metestrus/diestrus, proestrus or estrus during the four 2-week stages of increasing CR (stage 1: before CR; stage 2: weeks 1 & 2, 10-20% restriction; stage 3: weeks 3 & 4, 30-40% restriction; and stage 4: weeks 5 & 6, 40% restriction) for each genotype of the estrous cycle during the 6-week cycling (n=6 for N-MUT, n=14 for WT, n=5 for N-OX). 2-way ANOVA indicates significant CR effect (p<0.0001) and significant interaction of CR and genotype (p=0.003) for met/diestrus, a CR effect (p<0.0001) for proestrus, and a genotype effect (p=0.017), a CR effect (p<0.0001), and a significant interaction of CR and genotype (p=0.011) for estrus. **B.** LH levels during the four stages of CR (n=6 for N-MUT, n=12 for WT, n=5 for N-OX). No significant differences were observed. C. FSH levels during the four stages of CR (n=6 for N-MUT, n=12 for WT, n=5 for N-OX). 2-way ANOVA indicates significant genotype effect (p=0.022) and CR effect (p=0.002) but no significant interaction. **D, E and F.** Estradiol, progesterone and testosterone levels before and after CR (n=3 for N-MUT, n=3 for WT, n=3 for N-OX, each sample was pooled from two animals). 2-way ANOVA indicates a significant genotype effect (p=0.0004) and CR effect (p=0.0033) for estradiol, a CR effect (p=0.0055) for progesterone, and a genotype effect (p=0.015) and CR effect (p=0.019) for testosterone. No

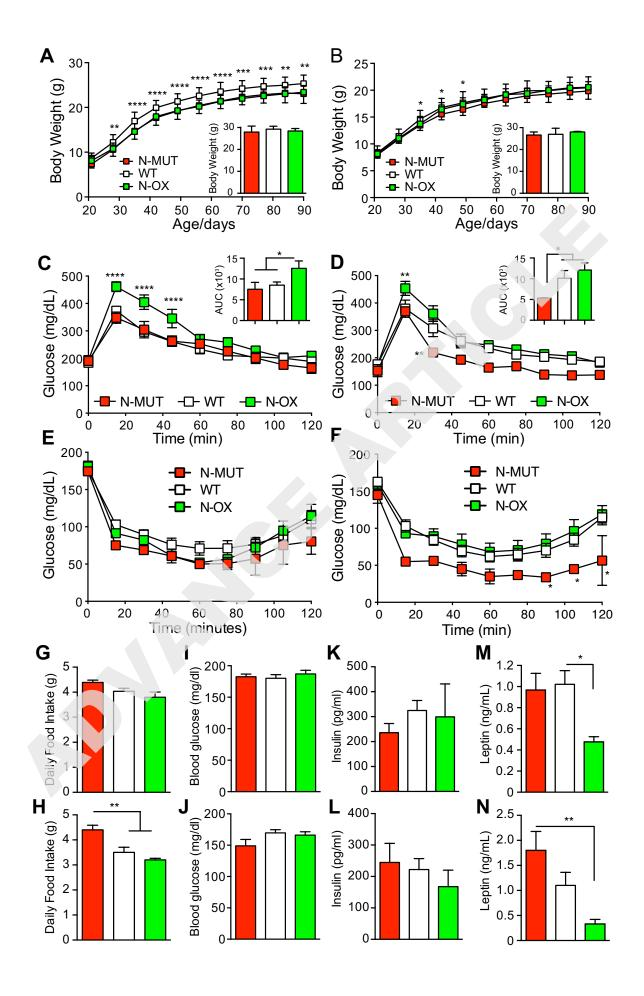
ADVANCE ARTICLE: JES JOURNAL DE

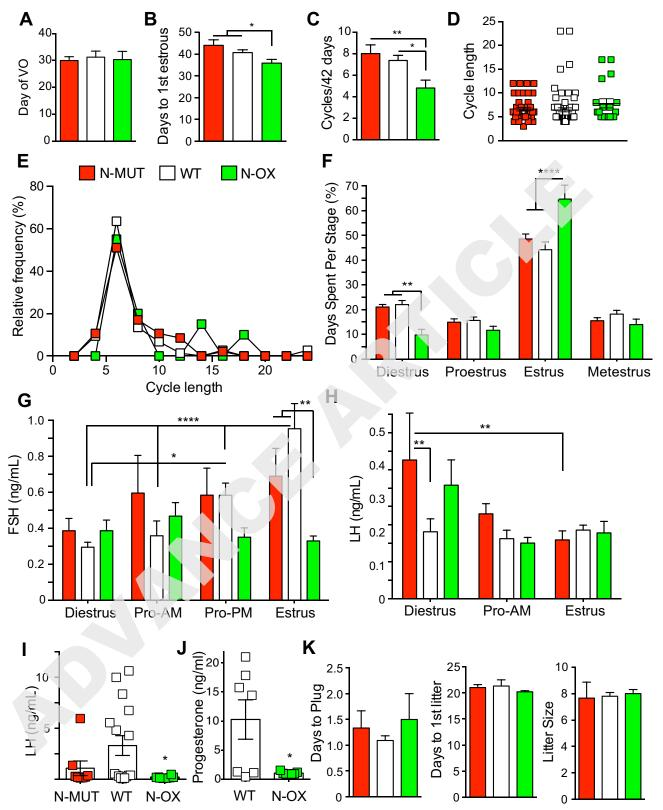
significant interactions of CR and genotype were observed. Asterisks indicate significant differences as indicated from post-hoc testing; *p<0.05, **p<0.01, *p<0.001, ****p<0.0001.

Figure 6: Hypothalamic and pituitary gene expression in N-MUT and N-OX mice. Color scheme is same as Figure 1. A. Gene expression in the hypothalami from female mice by QPCR. B. Gene expression in the pituitaries from female mice by QPCR. Data are shown as mean \pm SEM, n=5 for N-MUT, n=10 for WT, and n=5 for N-OX. Asterisks indicate statistical significance as indicated by ANOVA: *p<0.05, **p<0.01.

Figure 7: Metabolic cage assessment of N-OX mice. WT mice (n=6) are shown in black and N-OX mice (n=6) in green. Graphs show diurnal patterns over 24 h measured per 13 minute interval. Horizontal black bar indicates period of lights off (6 pm to 6 am). **A.** Ambulatory activity counts (x-axis). **B.** Rearing activity counts (z-axis). **C.** VO₂ consumption (ml/kg/h). **D.** Respiratory exchange ratio (RER). **E.** Food intake (g). **F.** Water intake (ml). **G.** Heat produced (kcal/h). **H.** Cage Temperature (°C). Data are shown as mean ± SEM. In all cases repeated measures ANOVA indicated a significant time effect (p<0.0001). Ambulatory activity, rearing activity, VO2, RER, and water intake showed significant genotype effects (p<0.0001, p<0.0001, p<0.0001, p=0.0004, and p=0.04, respectively). Asterisks indicate statistical significance by post-hoc testing: *p<0.05, **p<0.01.







Downloaded from https://academic.oup.com/jes/advance-article-abstract/doi/10.1210/js.2018-00318/5257832 by guest on 29 December 2018

